

Synthesis of Novel Chiral L-Phenylalanine Grafted PEDOT Derivatives with Electrochemical Chiral Sensor for 3,4-Dihydroxyphenylalanine Discrimination

Dufen Hu, Baoyang Lu, Kaixin Zhang, Xiaoxia Sun, Jingkun Xu*, Xuemin Duan*, Liqi Dong, Hui Sun, Xiaofei Zhu and Shijie Zhen

School of Pharmacy, Jiangxi Science & Technology Normal University, Nanchang, 330013, P R China
*E-mail: xujingkun@tsinghua.org.cn; duanxuemin@126.com

Received: 4 January 2015 / Accepted: 5 February 2015 / Published: 24 February 2015

Two amino-functionalized chiral poly(3,4-ethylenedioxythiophene) (PEDOT) derivatives, poly(*N*-(*tert*-butoxycarbonyl)-L-phenylalanyl (3,4-ethylenedioxythiophene-2'-yl)methylamide) (PEDOT-Boc-Phe) and poly(L-phenylalanyl (3,4-ethylenedioxythiophene-2'-yl)methylamide) (PEDOT-Phe), were synthesized electrochemically via potentiostatic polymerization of corresponding monomers *N*-(*tert*-butoxycarbonyl)-L-phenylalanyl (3,4-ethylenedioxythiophene-2'-yl)methylamide (EDOT-Boc-Phe) and L-phenylalanyl (3,4-ethylenedioxythiophene-2'-yl)methylamide (EDOT-Phe). The electrochemical behavior, structural characterization, spectroscopic properties, and surface morphology of two chiral conducting polymer films were systematically explored. They displayed excellent reversible redox activities, and rough and compact surface. Importantly, PEDOT-Boc-Phe and PEDOT-Phe modified electrodes were used to identify 3,4-dihydroxyphenylalanine (DOPA) enantiomers by square wave voltammetry (SWV) in sulphuric acid solution. It is interesting that the SWV peak currents of enantiomers were found to be quite different and hence the enantiomers could be successfully recognized but the enantioselectivity was not observed using the common method of cyclic voltammetry (CV). Satisfactory results implied that the obtained polymer films could play crucial roles in the development of practical value and analytical application prospects.

Keywords: Chiral poly(3,4-ethylenedioxythiophene); Amino acids; Chiral sensors; Square wave voltammetry; 3,4-Dihydroxyphenylalanine enantiomers

1. INTRODUCTION

In recent years, there has been paid more attention to the development of chiral conducting polymers for their potential applications in material science, chemical and biological sensors [1,2], catalysis, pharmaceuticals, enantioselective separation [3], and so on [4-8]. Therefore, a series of

new-generation chiral conducting polymers with multifunctional and high-performance have been designed and synthesized to explore their promising potential applications. Poly(3,4-ethylenedioxythiophene) (PEDOT) has emerged as one of the most promising conducting polymers of polythiophene (PTh) series, which especially stands out in the field of electroactive and conducting polymers for its exemplary properties such as high electrical conductivity, low band gap, good redox activity, thermal stability, long-term stability, and excellent transparency in the doped state. Chiral PEDOT is a representative branch of PEDOT family, which has attracted considerably widespread interest due to its fascinating properties such as optically activity and helical structure. Chiral PEDOTs were initially reported by Caras-Quintero and Bäuerle [9] by substituting different moieties at the ethylene bridge [10]. Recently, Akagi and co-workers [11-15] have developed an electrochemical polymerization method with chiral nematic liquid crystal as an electrolyte, and successfully used the method to produce unsubstituted chiral PEDOT. The same group also put forward that the chirality and electrochromism of chiral PEDOT derivatives can be controlled by changing the polymer structures between the doped and dedoped states through electrochemical doping and dedoping processes [12]. In addition, grafting chiral moieties onto the side chain to obtain novel chiral PEDOT derivatives has also attracted highly attention by many research institutions worldwide. Hence, natural amino acids can be used as the ideal chiral materials to obtain chiral PEDOTs by attaching them onto PEDOT side chain [16,17]. Furthermore, to the best of our knowledge, the field of using the property of chiral PEDOT for the enantiomeric recognition is still very rare [18].

3,4-Dihydroxyphenylalanine (DOPA) is a well-characterized reducing agent and a major product of hydroxyl radical addition to free tyrosine. Due to the particularity of DOPA structure, it has L- and D- two kinds of configurations. L-DOPA is the precursor to neurotransmitters, dopamine, norepinephrine (noradrenaline), and epinephrine (adrenaline), collectively known as catecholamines. Importantly, L-DOPA has been widely used in the treatment of Parkinson's disease for more than forty years and it plays a very crucial role in clinic and neurochemistry [19-21]. In addition, L-DOPA can be produced employing chemical, enzymatic, or microbial processes [22-24]. Nevertheless, its antipode, D-DOPA is inactive and has toxic properties [25,26]. Owing to different metabolisms of the active and inactive components, using racemic mixtures containing D- and L-DOPA may cause serious side effects [27,28]. Therefore, the study of chiral recognition of DOPA enantiomers is very important in chemical biology and pharmacology significance. In the past few years, a variety of methods have been proposed for the enantioseparation and determination of DOPA, such as high-performance liquid chromatography [29-31], capillary electrophoresis [32-34], tandem mass spectrometry [35], electrochemical methods [36-38], *etc.* In comparison with these methods, electrochemical methods, which have the advantages of low cost, high speed and high sensitivity, are always regarded as the lowest cost effective ratio for the discrimination of DOPA.

In this work, L-phenylalanine was chosen as the side chain moiety into EDOT through covalent bonding. Two novel PEDOT derivatives, poly(*N*-(*tert*-butoxycarbonyl)-L-phenylalanyl (3,4-ethylenedioxythiophene-2'-yl)methylamide) (PEDOT-Boc-Phe) and poly(L-phenylalanyl (3,4-ethylenedioxythiophene-2'-yl)methylamide) (PEDOT-Phe), were electrosynthesized for the first time through electropolymerization of the corresponding EDOT derivatives of *N*-(*tert*-butoxycarbonyl)-L-phenylalanyl (3,4-ethylenedioxythiophene-2'-yl)methylamide (EDOT-Boc-Phe) and L-phenylalanyl (3,4-

ethylenedioxythiophene-2'-yl)methylamide (EDOT-Phe), which were synthesized by acylation reaction. The electrochemical behavior, structural characterization, solubility, spectroscopic properties, thermal stabilities, and surface morphology of the as-prepared PEDOT-Boc-Phe and PEDOT-Phe films were investigated in detail. In addition, chiral PEDOT-Boc-Phe and PEDOT-Phe modified glassy carbon electrodes (GCEs) were used to recognize enantiomers of DOPA by methods of cyclic voltammetry (CV) and square wave voltammetry (SWV) in 0.25 mol L⁻¹ H₂SO₄ solution.

2. EXPERIMENTAL DETAILS

2.1 Materials

Enantiomerically pure 3,4-dihydroxyphenylalanine (DOPA, 99%), L-phenylalanine (99%), N₃-dimethylpropane-1,3-diamine (EDC, 99%), N-hydroxybenzotriazole (HOBT, 99%), trifluoroacetic acid (TFA, 99%), sulfuric acid (H₂SO₄, 98%), and di-*tert*-butyl dicarbonate ((Boc)₂O, 99%) were purchased from Aladdin Chemistry Co. Ltd. and dimethyl sulfoxide (DMSO, AR) was purchased from Tianjin Bodi Chemicals Co., Ltd. Dichloromethane (CH₂Cl₂, AR; Tianjin Damao Chemical Reagent Factory) was purified by distillation over calcium hydride before used. *Tetra-n*-butylammonium hexafluorophosphate (Bu₄NPF₆, 99%; Acros Organics) was dried under vacuum at 60 °C for 24 h before used. 2'-Aminomethyl-3,4-ethylenedioxythiophene (EDOT-MeNH₂) was prepared in accordance with our previous procedure [16,39,40].

2.2 Syntheses

2.2.1 *N*-(*tert*-butoxycarbonyl)-L-Phenylalanine (*N*-Boc-L-Phe)

A solution of (Boc)₂O (2.62 g, 12 mmol) in dioxane (10 mL) was added to an ice-cold solution of L-phenylalanine (1.65 g, 10.00 mmol) in 1 M NaOH (21 mL) with stirring at -5 °C. After 30 min, the mixture was stirred for over 14 h at room temperature. The mixture was concentrated to half its original volume by rotary evaporation, cooled in ice, and acidified pH to 2-3 by slow addition of 1 M NaHSO₄. Finally, the solution was extracted with acetic ether (3 × 25 mL), and the combined organic layer were dried with anhydrous MgSO₄, and concentrated to give 2.28 g of a colorless solid (yield 86%)

2.2.2 EDOT-Boc-Phe

EDOT-MeNH₂ (0.86 g, 5 mmol), EDC (1.15 g, 6 mmol), and HOBT (0.05 g, 0.37 mmol) were dissolved in CH₂Cl₂ (22 mL) with stirring while being cooled in an ice bath. A solution of *N*-Boc-L-Phe (1.59 g, 6 mmol) in CH₂Cl₂ (22 mL) was added slowly. After stirring for 1 h, the ice bath was removed and the reaction was performed with continued stirring at room temperature for another 16 h. Subsequently, the colorless reaction solution was washed with 1 M HCl (3 × 50 mL), a saturated

solution of NaHCO_3 (3×50 mL), and then with saturated brine (1×50 mL), respectively. The organic layer was dried with anhydrous MgSO_4 . The solvent was removed under reduced pressure and the remaining crude product was isolated by flash chromatography (silica gel, petroleum ether/ethyl acetate, 2/1, v/v) to give 1.90 g of a colorless solid (yield 91%). $[\alpha]_D^{20} = -0.718^\circ$. ^1H NMR (400 MHz, $\text{DMSO}-d_6$, ppm): δ 8.23 (t, $J = 6.8$ Hz, 1H), 7.25 (s, 4H), 7.18 (s, 1H), 6.99 (d, $J = 7.2$ Hz, 1H), 6.58 (s, 2H), 4.02-4.14 (m, 3H), 3.72-3.85 (m, 1H), 3.33 (t, $J = 14.0$ Hz, 2H), 2.92 (d, $J = 13.2$ Hz, 1H), 2.75 (t, $J = 11.6$ Hz, 1H), 1.17-1.30 (m, 9H).

2.2.3 EDOT-Phe

EDOT-Boc-Phe (1.20 g, 2.87 mmol) was dissolved in CH_2Cl_2 (50 mL) with stirring while being cooled in an ice bath. A solution of TFA (2.75 mL) in CH_2Cl_2 (6 mL) was added slowly. After 5 h, the pH of the mixture was adjusted to basicity with a saturated solution of NaHCO_3 . Then the mixture was extracted with CH_2Cl_2 (3×150 mL), and saturated brine (3×150 mL), respectively. The organic layer was dried with anhydrous MgSO_4 . The solvent was removed under reduced pressure and the remaining crude product was isolated by flash chromatography (silica gel, dichloromethane/methanol, 32/1, v/v) to give 0.63 g of a colorless solid (yield 69%). $[\alpha]_D^{20} = -28.527^\circ$. ^1H NMR (400 MHz, $\text{DMSO}-d_6$, ppm): δ 7.67 (d, $J = 5.6$ Hz, 1H), 7.22-7.34 (m, 5H), 6.34 (s, 2H), 4.18-4.24 (m, 2H), 3.91-3.78 (m, 1H), 3.65-3.68 (m, 2H), 3.44-3.58 (m, 1H), 3.27-3.25 (m, 1H), 2.72-2.74 (m, 1H).

2.3 Electrochemical measurements

Electrochemical synthesis and examination were performed in a one-compartment cell with the use of Model 263A potentiostat-galvanostat (EG&G Princeton Applied Research) under a computer control. The three electrodes of the working electrode, the reference electrode, and the counter electrode were all platinum (Pt) wires with a diameter of 0.5 mm, which were placed 5 mm apart in the transverse direction during the measurements. Besides, to obtain a sufficient amount of polymer for characterization, the Pt sheets with surface area of 10 and 12 cm^2 each (10 mm apart) were employed as working and counter electrodes, respectively, the Pt wire electrode directly immersed in the solution served as the reference electrode and it also revealed sufficient stability during the experiments. Electrodes mentioned above were carefully polished with abrasive paper (1500 mesh). All experiments were carried out under a slight argon overpressure. Finally, the polymer films were dried at 60 $^\circ\text{C}$ under vacuum for 24 h. The PEDOT-Boc-Phe film was prepared in CH_2Cl_2 - Bu_4NPF_6 (0.10 M) containing 0.01 M EDOT-Boc-Phe and characterized electrochemically in monomer-free CH_2Cl_2 - Bu_4NPF_6 (0.10 M). The PEDOT-Phe film was prepared in CH_2Cl_2 - Bu_4NPF_6 (0.10 M) containing 3% TFA and 0.01 M EDOT-Phe and characterized electrochemically in monomer-free CH_2Cl_2 - Bu_4NPF_6 (0.10 M) containing 3% TFA. Both PEDOT-Boc-Phe and PEDOT-Phe films were dedoped by 25% ammonia for three days. After dedoping, their color both changed to brownish yellow.

2.4 Fabrication of sensor

The glassy carbon electrode (GCE) with a diameter of 3 mm served as the working electrode, and two Pt wires with a diameter of 0.5 mm were used as the counter electrode and the reference electrode. The counter electrode was carefully polished with abrasive paper (1500 mesh). The GCE was polished with alumina (Al_2O_3 , 0.05 μm). Then, the counter electrode and the GCE was ultrasonically cleaned in turn with deionized distilled water, ethanol, and deionized distilled water each for 5 min, respectively. Then, they were dried in air before the experiment. Three electrodes in the cell were placed 5 mm apart during electrochemical measurements. To fabricate a sensor, a GCE electrode was used as the working electrode, a platinum wire as an auxiliary electrode and a saturated calomel reference electrode (SCE). The PEDOT-Boc-Phe film was performed by the chronoamperometry (I-t) method at 1.5 V in CH_2Cl_2 at room temperature in a one-compartment three-electrode cell. And the PEDOT-Phe film was performed by the I-t method at 1.0 V in CH_2Cl_2 containing 3% TFA in a one-compartment three-electrode cell. The obtained PEDOT-Boc-Phe and PEDOT-Phe modified GCE electrodes were washed repeatedly with CH_2Cl_2 to remove the electrolyte and monomer, and dried in air.

2.5 Characterization

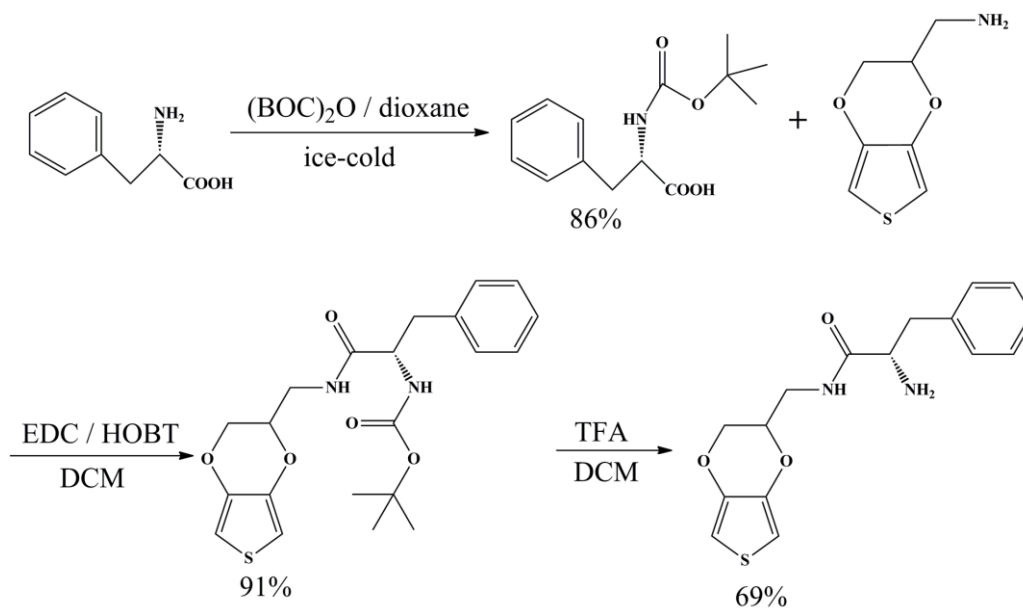
NMR spectra were recorded on a Bruker AV 400 NMR spectrometer with d_6 -DMSO as the solvent and tetramethylsilane (TMS, singlet, chemical shift: 0.0 ppm) as an internal standard. Infrared spectra (IR) were recorded using Bruker Vertex 70 Fourier spectrometer with samples in KBr pellets. Ultraviolet-visible (UV-*vis*) spectra were measured with a Perkin-Elmer Lambda 900 ultraviolet-visible-near-infrared spectrophotometer. Optical rotation determination was performed on Anton Paar MCP 200 polarimeter. Fluorescence spectra of the monomers and polymers were determined with an F-4500 fluorescence spectrophotometer (Hitachi). Scanning electron microscopy (SEM) measurements were taken using Sigma cold field emission scanning electron microscope. The addition of solutions to the cell was performed with the Finnpiquette (Labsystems, Helsinki, Finland). The temperature was controlled with a type HHS thermostat (Shanghai, China).

3. RESULTS AND DISCUSSION

3.1 Syntheses of monomers

There are two routes to introduce amino acids into EDOT side chain. One is using the carboxyl group of amino acids and 2'-hydroxymethyl-3,4-ethylenedioxythiophene (EDOT-MeOH) to form ester bond. However, it found that the obtained ester would be hydrolyzed in short time after removing the Boc group on amino in the experimental process, which attributes to the existence of its own amino group.¹⁷ Hence, another route was explored to synthesize EDOT-Phe efficiently in this work (Scheme 1). EDOT-Boc-Phe was made according to the reported method investigated by McTiernan *et al* [41].

Because strong acids can destroy the ether linkage of EDOT, TFA was chosen to remove Boc group on the EDOT-Boc-Phe to get EDOT-Phe monomer. In this work, the synthetic route of monomers was showed in Scheme 1.



Scheme 1 Efficient synthesis routes for EDOT-Boc-Phe and EDOT-Phe.

3.2 Electrochemical polymerization of EDOT-Boc-Phe and EDOT-Phe

The polymers were electrosynthesized in $\text{CH}_2\text{Cl}_2\text{-Bu}_4\text{NPF}_6$ (0.10 M) system containing 0.01 M monomers (3% TFA were added to the monomer of EDOT-Phe mixture solutions). The addition of TFA during the electrochemical polymerization of EDOT-Phe could suppress the oxidation of amino group, and decrease the onset oxidation potential of corresponding monomer. As can be seen from Fig. 1, all the cyclic voltammograms (CVs) showed similar characteristics to those of other inherently conducting polymers, which indicated that the polymerization processed easily even at low monomer concentrations. In the first cycle of CVs, the current density on the reverse scan was higher than that on the forward scan (in the region of -0.75 V to 1.45 V (EDOT-Boc-Phe) and -0.3 V to 1.0 V (EDOT-Phe)). Comparing with these two figures, the formation of this loop could be explained as the characteristics of nucleation process [42-45]. In Fig. 1A, during the oxidative scan, one oxidation peak appeared at 0.51 V and one reduction peak appeared at -0.074 V, and in Fig. 1B, the redox peaks appeared at 0.64 V and -0.15 V, respectively. All these peaks were attributed to the *p*-doping/dedoping processes of PEDOT-Boc-Phe and PEDOT-Phe films formed in previous scans. Upon sequential cycles, the redox currents increased, implying that the formation of an electroactive and conductive layer on the Pt electrode surface (light-blue to blue-black as the deposit thickened) was gradually increasing. Moreover, the broad redox waves of the as-formed PEDOT-Boc-Phe and PEDOT-Phe films could be ascribed to the wide distribution of the polymer chain length or the version of conductive species on the polymer main chain from the dedoped state to polarons, from polarons to bipolarons, and finally from bipolarons to the metallic state [46]. The potential shift of the current

wave maximum provided information about the increase of the electrical resistance of the polymer films and the overpotential needed to overcome this resistance.

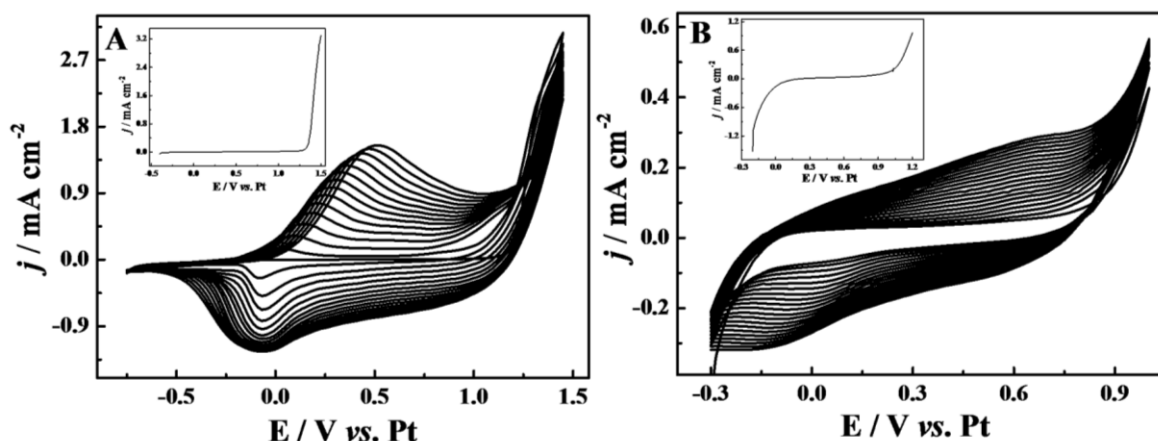


Figure 1. Cyclic voltammograms (CVs) of EDOT-Boc-Phe (A) in $\text{CH}_2\text{Cl}_2\text{-Bu}_4\text{NPF}_6$ (0.1 M) and EDOT-Phe (B) in $\text{CH}_2\text{Cl}_2\text{-Bu}_4\text{NPF}_6$ (0.1 M) containing 3% TFA. Monomer concentration: 0.01 M. Potential scan rate: 100 mV s^{-1} .

Potentiostatic synthesis was employed to prepare PEDOT-Boc-Phe and PEDOT-Phe films. Considering the overall factors affecting the quality of the formed films, such as moderate polymerization rate, negligible overoxidation, regular morphology, and good adherence against the working electrode, the selected applied potentials were 1.5 V and 1.0 V for the electropolymerization of EDOT-Boc-Phe and EDOT-Phe, respectively.

3.3 Electrochemistry of PEDOT-Boc-Phe and PEDOT-Phe films

For insight into the electroactivity of the obtained polymer films, the electrochemical behavior of PEDOT-Boc-Phe and PEDOT-Phe films-modified electrodes were investigated by cyclic voltammetry (CV) in monomer-free $\text{CH}_2\text{Cl}_2\text{-Bu}_4\text{NPF}_6$ (Fig. 2). It was clearly seen that modified electrodes represented steady-state and broad redox peaks in monomer-free electrolytes. This might be ascribed to the presence of slow diffusion of the counterions inside the films, changes of the films capacitance, and a wide distribution of the polymer chain length resulting from coupling defects distributed statically [47]. The peak current densities were linearly proportional to the potential scanning rates (inset in Fig. 2), indicating that the redox processes were non-diffusional and the electroactive polymer films were well adhered to the working electrodes surface. Furthermore, the conversion between the conducting (doped) and insulating (dedoped) state was no significant decomposition, which indicated that the materials had high electrochemical stabilities.

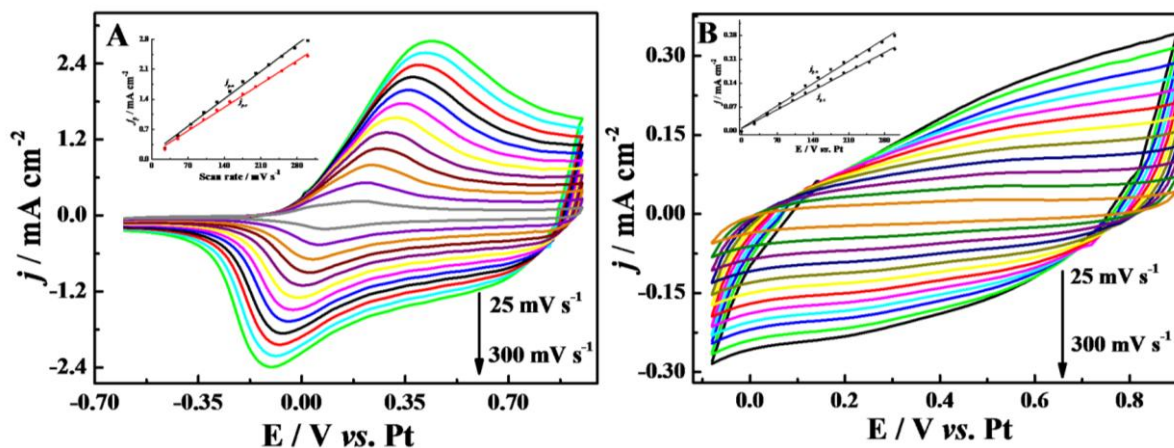


Figure 2. Cyclic voltammograms (CVs) of PEDOT-Boc-Phe (A) and PEDOT-Phe (B, containing 3% TFA) films in CH₂Cl₂–Bu₄NPF₆ (0.1 M) at a potential scan rates of 25, 50, 75, 100, 125, 150, 175, 200, 225, 250, 275 and 300 mV s⁻¹. The films were obtained by CV. Inset: plots of redox peak current densities vs. potential scan rates. j_p is the peak current densities, $j_{p,a}$ and $j_{p,c}$ denote the anodic and the cathodic peak current densities, respectively.

3.4 Optimization of electrical conditions and preparation of PEDOT-Boc-Phe and PEDOT-Phe

Potentiostatic electrolysis was employed to prepare the newly obtained PEDOT-Boc-Phe and PEDOT-Phe for characterization. To optimize the applied potential for polymerization, a set of current transients during the electropolymerization of PEDOT-Boc-Phe and PEDOT-Phe at different applied potentials in CH₂Cl₂ were recorded, as shown in Fig. 3. Typically, at applied potentials below the onset oxidation potential, no polymer films were formed on the electrodes, indicating that polymerization didn't occur on the electrode surface due to the low deposition voltage. Once the applied potential reached the threshold value, all the electrosynthetic current densities experienced an initial sharp increase followed by a slow decrease. The current density eventually became constant as a result of the uniform deposition of the polymer film on the electrode surface. At relatively high potentials, however, the surfaces of the polymer films became rough, discontinuous, and heterogeneous. Even worse, some films even fall into the solution from the electrode surface during/after the experiments. This phenomenon was mainly due to significant overoxidation at higher potentials, which led to poor quality films. Considering the overall factors affecting the quality of the as-formed polymer films, such as moderate polymerization rate, negligible overoxidation, regular morphology, and good adherence against the working electrode, the optimized applied potential for PEDOT-Boc-Phe was 1.5 V vs. Pt. And the optimized applied potential for PEDOT-Phe was 1.1 V vs. Pt. Therefore, PEDOT-Boc-Phe and PEDOT-Phe films used for the characterization mentioned below were all prepared by the chronoamperometry method at the constant potential of 1.5 V and 1.1 V vs. Pt in CH₂Cl₂, respectively.

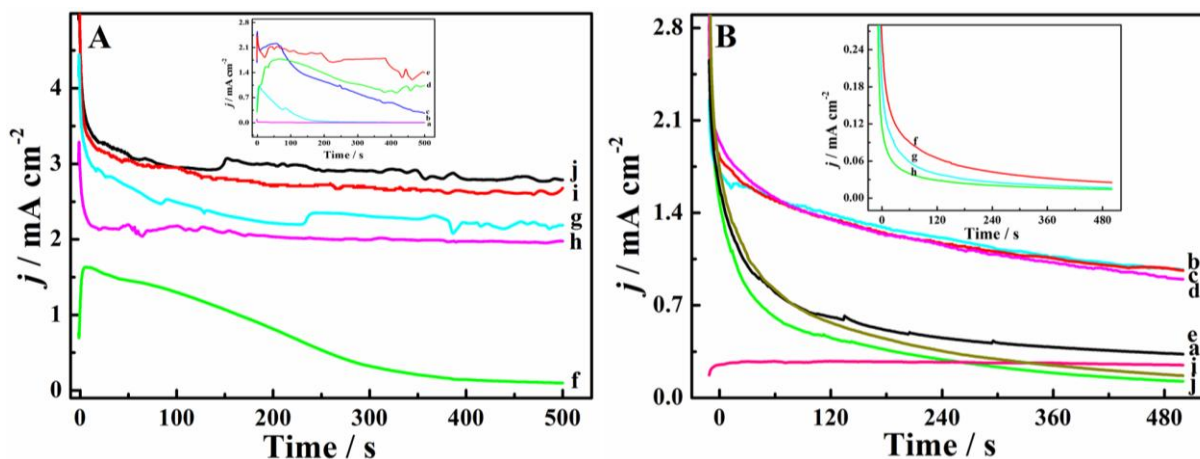


Figure 3-A Chronoamperometric response of EDOT-Boc-Phe electropolymerization on three Pt electrodes for films prepared in 0.01 mol L⁻¹ EDOT-Boc-Phe in CH₂Cl₂-Bu₄NPF₆ (0.1 M) by applying 1.10, 1.15, 1.20, 1.25, 1.30, 1.35, 1.40, 1.45, 1.5 and 1.55 V, respectively.-**B** Chronoamperometric response of EDOT-Phe electropolymerization on three Pt electrodes for films prepared in 0.01 mol L⁻¹ EDOT-Phe in CH₂Cl₂-Bu₄NPF₆ (0.1 M) containing 3% TFA by applying 0.8, 0.85, 0.9, 0.95, 1.0, 1.05, 1.10, 1.15, 1.20 and 1.25 V, respectively.

3.5 Infrared spectra

Vibrational spectra can provide much structural information for conducting polymers, especially for insoluble and infusible polymers. A comparison of the evolution of the vibrational modes appearing in conducting polymers and in some simpler related molecules acting as references usually facilitates the interpretation of the experimental absorption spectra. IR spectra of the monomers (a), and dedoped (b) polymers were illustrated in Fig. 4. The details of the band assignments for monomers, and polymers were given in Table 1. These peaks at 3106 cm⁻¹ for EDOT-Boc-Phe and 3108 cm⁻¹ for EDOT-Phe (Fig. 4A-a and 4B-a) were produced by C-H vibration of the α, α' -positions in the thiophene ring. These peaks were retained in the monomers but disappeared in the electrochemical polymerized samples (Fig. 4A and 4B). This indicated that the electropolymerization of EDOT occurred at the 2,5-positions of the thiophene ring. And the C-H vibration of the phenyl group was multiplet, and these peaks at 3106 cm⁻¹ for EDOT-Boc-Phe and 3108 cm⁻¹ for EDOT-Phe were single peak. These phenomenon indicated that these peaks at 3106 cm⁻¹ for EDOT-Boc-Phe and 3108 cm⁻¹ for EDOT-Phe were not the the C-H vibration of the phenyl group. From Fig. 4 and Table 1, the C=O stretching vibration existed in the spectra of monomers and polymers, indicating that the C=O double bond was not destroyed during electrochemical polymerization. Besides, N-H stretching vibration of monomers and polymers also displayed (Fig. 4A and 4B). The peak at 3366 cm⁻¹ was the vibration bands of N-H and NH₂ stretching of the monomer (Fig. 4B-a), which were shifted to 3342 cm⁻¹ in the dedoped polymer (Fig. 4B-b).

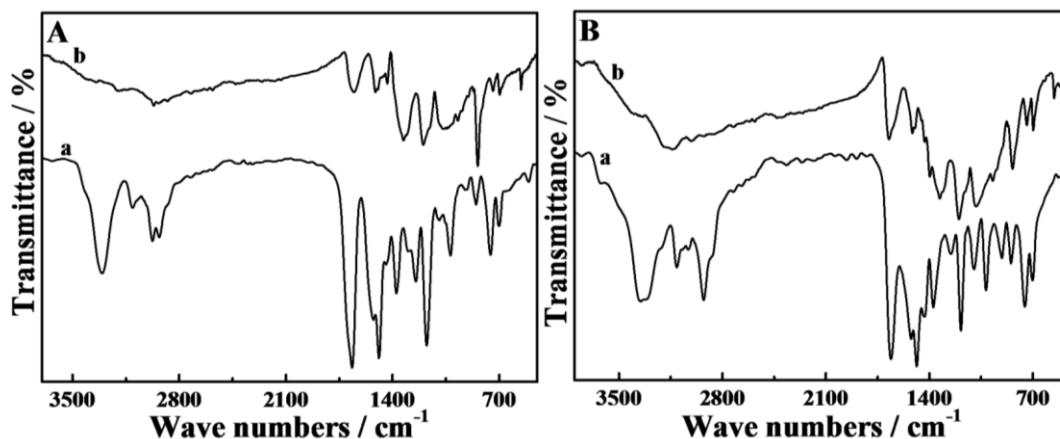


Figure 4. FT-IR spectra of monomers and polymers: EDOT-Boc-Phe (A-a), dedoped PEDOT-Boc-Phe (A-b), EDOT-Phe (B-a), and dedoped PEDOT-Phe (B-b).

Table 1. Assignments of IR Spectra of monomers (EDOT-Boc-Phe and EDOT-Phe) and polymers (PEDOT-Boc-Phe and PEDOT-Phe)

| EDOT-Boc-Phe | | EDOT-Phe | |
|---|-----------------------------|--------------------------|-----------------------------|
| band (cm ⁻¹) | assignment | band (cm ⁻¹) | assignment |
| 3117 (a), 1665 (a), 1519 (a), 1176 (a); 1652 (b), 1512 (b), 1329 (b) | N-H stretching vibration | 3336 (a), 3408 (b) | N-H stretching vibration |
| 1679 (a), 1673 (b) | C=O stretching vibration | 1665 (a), 1677 (b) | C=O stretching vibration |

All results confirmed that structures of EDOT-Boc-Phe and EDOT-Phe were not destroyed during the electrochemical polymerization process. Moreover, the augmented width and shifts of these bands from the monomer to polymer manifested the occurrence of the electrochemical polymerization. The broadening of the IR bands in the experimental spectra was due to the resulting product composed of oligomers with wide chain dispersity. The vibrational peaks of the oligomers with different polymerization degrees had different IR shifts. These peaks overlapped one another and produced broad band with hyper-structures. Furthermore, there were chemical defects on the polymer chains, which resulted from the inevitable overoxidation of the polymers. This also contributed to the band broadening of IR spectra [48].

3.6 UV-vis and fluorescent spectra

PEDOT-Boc-Phe film prepared from CH₂Cl₂-Bu₄NPF₆ in the doped state with dark brown color. While PEDOT-Phe film prepared in CH₂Cl₂-Bu₄NPF₆ containing 3% TFA were in the doped state with dark brown color. When they were dedoped by 25% ammonia for three days, their color both changed to brownish yellow. It is very interesting that both dedoped PEDOT-Boc-Phe and

PEDOT-Phe films are partly soluble in many common organic solvents, such as acetonitrile, DMSO, dichloromethane, tetrahydrofuran, and chloroform, *etc.*

UV–vis spectra of the monomers and corresponding polymer films dissolved in DMSO were illustrated in Fig. 5. The EDOT-Boc-Phe monomer showed a characteristic absorption peak at 264 nm (Fig. 5A-a), while the spectra of the doped and dedoped PEDOT-Boc-Phe film showed two much broader absorptions with their maximum at 550 nm (Fig. 5A-b) and 570 nm (Fig. 5A-c), respectively. In comparison, EDOT-Phe monomer presented a characteristic absorption peak at 260 nm (Fig. 5B-a) and the doped PEDOT-Phe film showed absorption at 568 nm (Fig. 5B-b) and dedoped PEDOT-Phe film presented absorption at 565 nm (Fig. 5B-c). The overall absorption of PEDOT-Boc-Phe and PEDOT-Phe tailed off to more than 700 nm (Fig. 5A and 5B). Generally, longer wavelength in spectra indicated longer polymer sequence [49]. These spectral results confirmed the occurrence of the electrochemical polymerization among the monomer and the formation of a conjugated polymer with broad molar mass distribution.

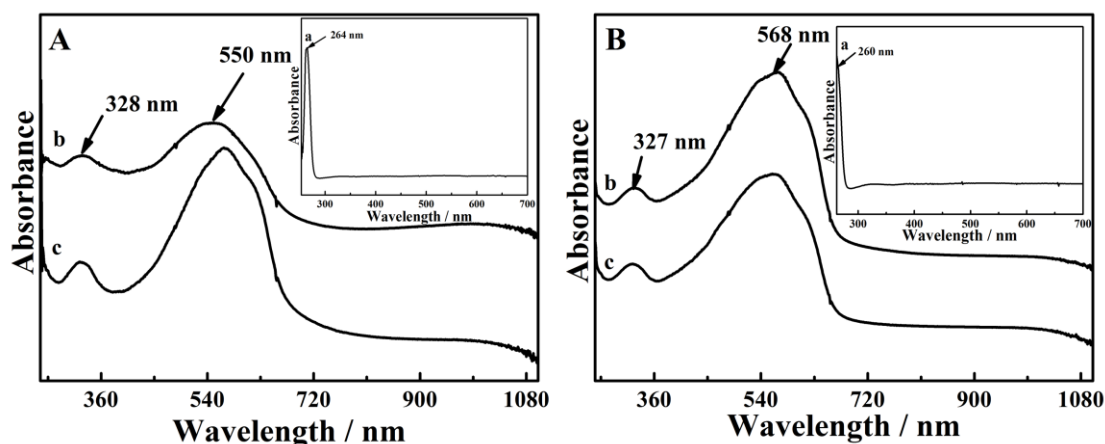


Figure 5. UV–vis spectra of monomers and polymers: EDOT-Boc-Phe (A-a), doped PEDOT-Boc-Phe (A-b), dedoped PEDOT-Boc-Phe (A-c), EDOT-Phe(B-a), doped PEDOT-Phe (B-b) and dedoped PEDOT-Phe (B-c). The monomers and polymers were dissolved in DMSO.

The fluorescence spectra of the monomers and corresponding polymer films in DMSO were also recorded (Fig. 6). It was observed that the emission peak of EDOT-Boc-Phe emerged at 350 nm, whereas the dominant maximum emission was at 657 nm for dedoped PEDOT-Boc-Phe. Meanwhile, the emission peak of the monomer of EDOT-Phe occurred at 352 nm with a small shoulder, while the dominant maximum emission at 650 nm characterized the spectra of the dedoped PEDOT-Phe (Fig. 6B-b). It was obviously observed that the red shifts between monomers and polymers (about 300 nm) could be clearly seen from Fig. 6, which was mainly attributed to the elongation of the polymers delocalized π -electron chain sequence. This further proved the formation of the conjugated backbone of PEDOT-Boc-Phe and PEDOT-Phe, in accordance with UV–vis spectral results. These results also demonstrated that the polymers were orange-red-light emitting materials.

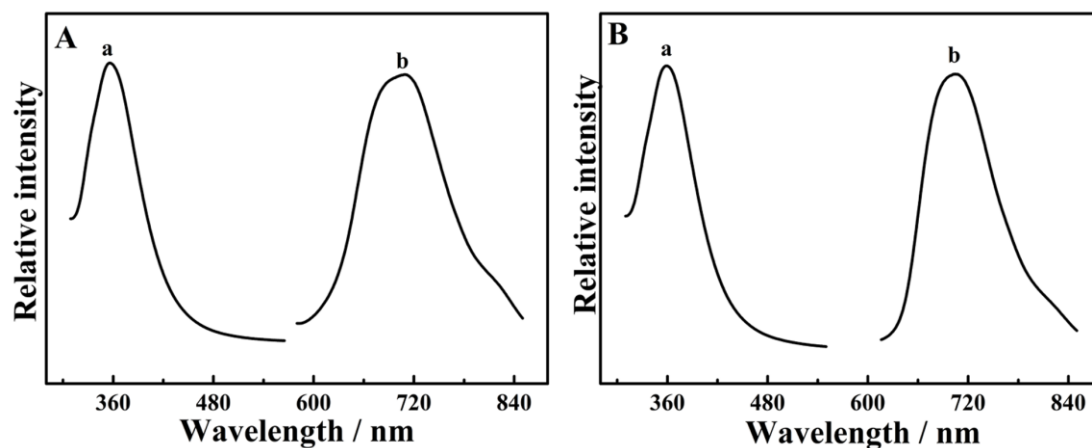


Figure 6. Fluorescence spectra of monomers and polymers: EDOT-Boc-Phe (A-a), dedoped PEDOT-Boc-Phe (A-b), EDOT-Phe (B-a), and dedoped PEDOT-Phe (B-b). The monomers and polymers were dissolved in DMSO.

3.7 Surface morphology

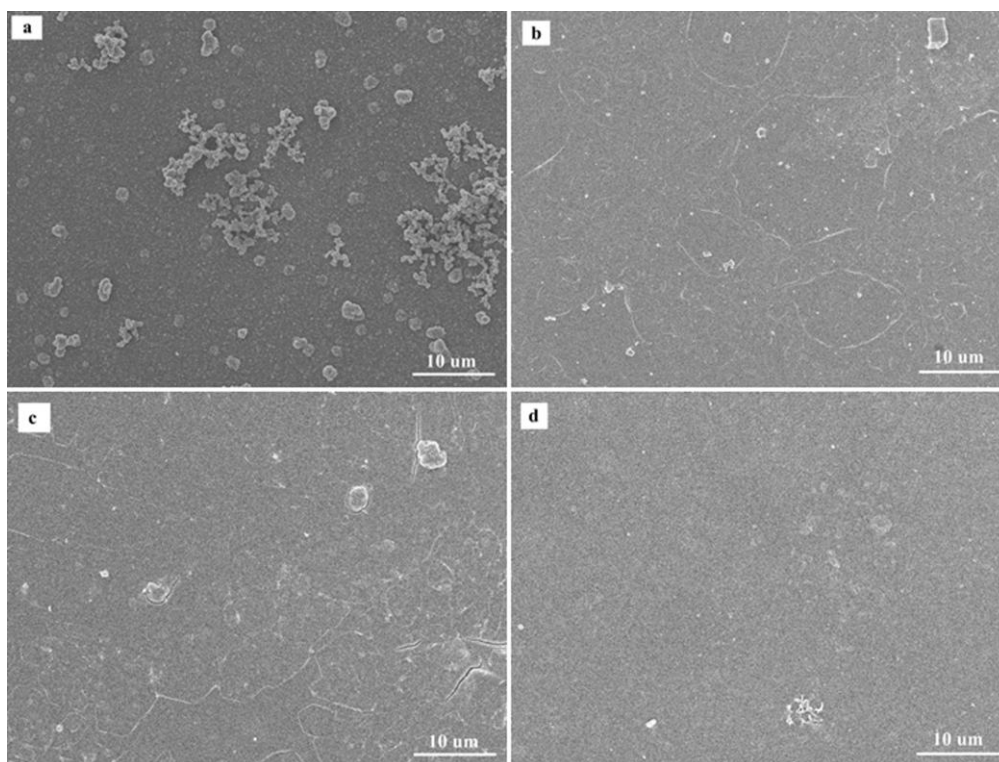


Figure 7. SEM photographs of PEDOT-Boc-Phe and PEDOT-Phe films deposited electrochemically on ITO electrode; doped and dedoped PEDOT-Boc-Phe (a and b); doped and dedoped PEDOT-Phe (c and d).

SEM was carried out in order to study the surface morphology of the conducting polymer films. There were no obvious differences in surface morphology of the doped/dedoped PEDOT-Boc-Phe films (Fig. 7a and 7b). After dedoping electrochemically (the counter anions migrate out of the

polymer film), the surface of dedoped PEDOT-Boc-Phe film (Fig. 7b) was still rather compact. The surface morphology of PEDOT-Phe films (Fig. 7c and 7d) was similar to PEDOT-Boc-Phe films, which maintained smooth and homogeneous surface both in the doped and dedoped states. The smooth and homogeneous morphology of compact PEDOT-Phe films was extremely beneficial to improve their electrical conductivity and electron transfer capability. These small differences between the doped and dedoped polymer films were mainly due to the migration of counteranions out of the polymer films and their gradual solubility from the electrode to the solution during the dedoping processes [50], which broke the relatively smooth surfaces of doped polymer films.

3.8 Application of chiral discrimination

The electrochemical behaviour of the enantiomeric pairs (D- and L-DOPA) were studied by CV and SWV, respectively. The detection system was very important to detection result. In order to obtain good results, the system of $0.25 \text{ mol L}^{-1} \text{ H}_2\text{SO}_4$ was chosen according to many reports [28,51-53]. There is no apparent Faradic response of DOPA at the bare glassy carbon electrode (GCE) in $0.25 \text{ mol L}^{-1} \text{ H}_2\text{SO}_4$ containing $0.5 \text{ } \mu\text{mol L}^{-1}$ L-DOPA (dashed line) or D-DOPA (solid line). This result might be due to the concentration of samples too low to be detected for the bare GCE. As shown in Fig. 8, when the GCEs were modified by chiral PEDOT-Boc-Phe and PEDOT-Phe, two pairs of significant redox peaks were observed in the CV curves owing to two-electron-two-proton oxidation and reduction of DOPA/dopaquinone in this system. Also, the differences of CV peaks were too small to be distinguished between the enantiomers of DOPA, and thus D-/L-DOPA cannot be recognized with the CV technique in the same system. It presented that the sensitivity of PEDOT-Boc-Phe and PEDOT-Phe modified GCEs is better than bare GCE in the same situation. In addition, different results emerged using the SWV technique under the same conditions, the SWV peak currents for PEDOT-Boc-Phe of D-/L-DOPA are 9.6 and 11.2 μA , and the SWV peak currents for PEDOT-Phe 4.2 and 6.3 μA , respectively when the scanning potential of SWV was changed from low to high values (forward scan). In contrast, the peak currents for PEDOT-Boc-Phe are -10.5 and -10.3 μA , and the peak currents for PEDOT-Phe are -3.9 and -4.4 μA corresponding to D-/L-DOPA with a reverse scan, respectively. In Fig. 8b and 8d, it can be seen that obviously difference of SWV peaks was presented between D-/L-DOPA by SWV although it was very small. So the difference in SWV peaks may be sufficient to enable an accurate determination of the enantiomeric purity and composition of the DOPA analyte [28].

In $0.25 \text{ mol L}^{-1} \text{ H}_2\text{SO}_4$ containing $0.5 \text{ } \mu\text{mol L}^{-1}$ L-DOPA (dashed line) or D-DOPA (solid line), the DOPA enantiomers showed different SWV behaviours and thus enabled the sensor to convert the enantioselective recognition event into current changes. Basically, DOPA in the solution should exchange electrons with the GCE electrode after passing through the recognition layer. The electrochemical activity of DOPA was so good that the enantiomers cannot be distinguished by using common linear sweep voltammetry due to similar peaks. The waveform of SWV was a staircase scan, each tread of which was superimposed by a symmetrical double pulse, one in the forward direction and the other in the reverse. When SWV was applied in this case, the DOPA enantiomers may pass through

the chiral selectivity zone in a manner of oscillation, which would effectively extend the retention time. Each waveform scan made such an interaction time increase a little. After many cycles, the enantioseparation was finally amplified and thus the enantiomers were discriminated. In other words, SWV made limited recognition sites reused, which greatly increased the efficiency of chiral recognition. Meanwhile, PEDOT-Boc-Phe and PEDOT-Phe also acted as bidirectional switches, so the peaks of D- and L-DOPA were different with different potential scanning directions.

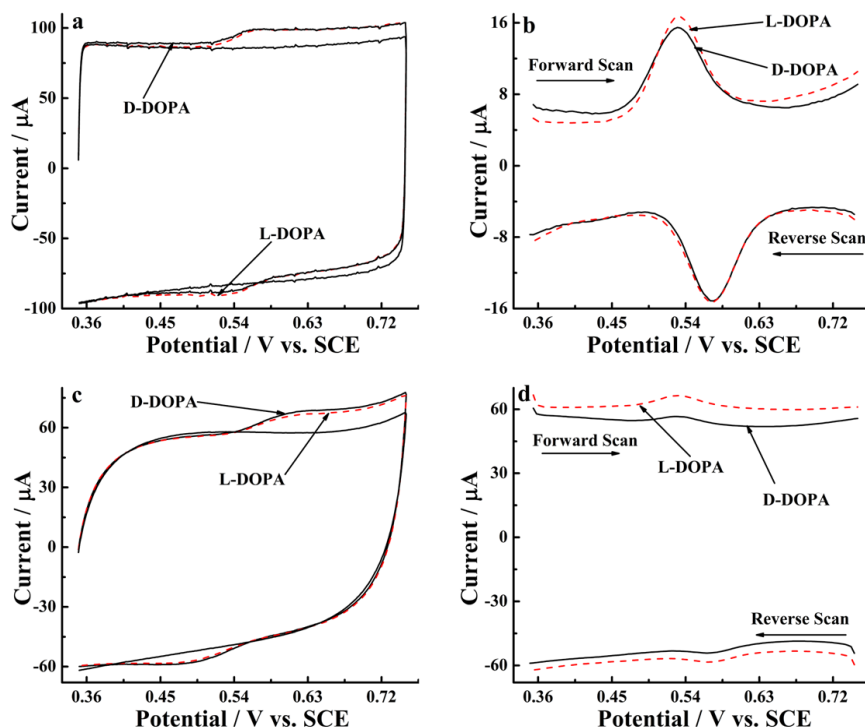
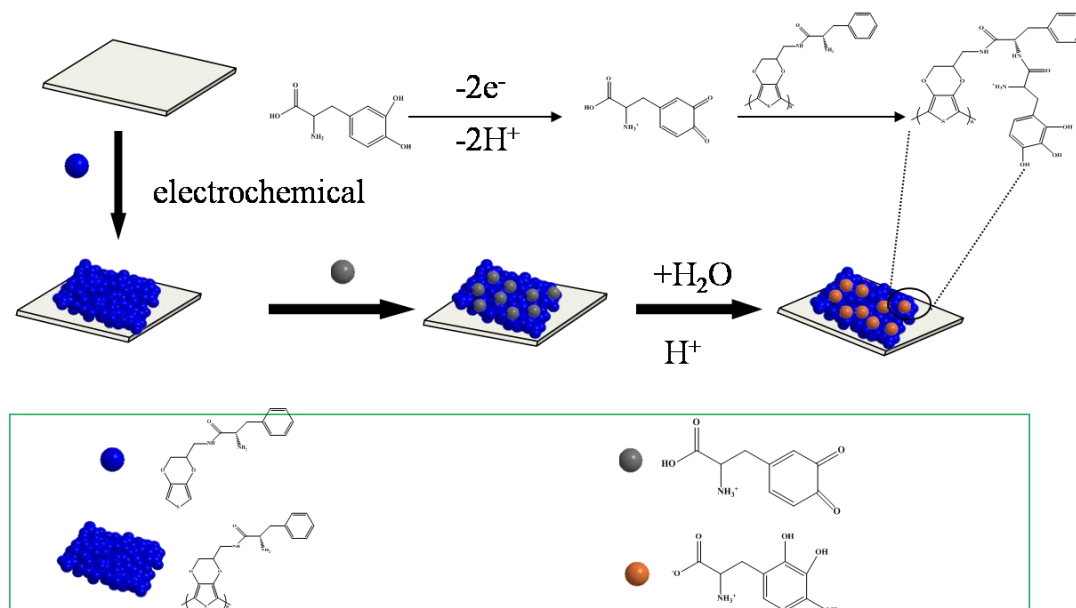


Figure 8. Cyclic voltammograms (CVs) (a and c) and SWVs (b and d) of PEDOT-Boc-Phe (a and b) and PEDOT-Phe (c and d) modified electrodes in $0.25 \text{ mol L}^{-1} \text{ H}_2\text{SO}_4$ containing $0.5 \text{ } \mu\text{mol L}^{-1}$ L-DOPA (dashed line) or D-DOPA (solid line). CV: scan rate, 50 mV s^{-1} ; SWV: step height, 0.004 V ; frequency, 1 Hz .

Brun and Rosset [51] showed that the redox response of L-DOPA solution was pH-dependent. Three provable mechanisms for the oxidation of DOPA were shown in Scheme 2. In parts of this Scheme, the DOPAquinone was consumed by hydrolysis, intramolecular and dimerization reaction, respectively. At low pHs, the amine and carboxyl groups would be protonated, and the molecules would be in acidic form. Therefore, the nucleophilic property of the amine group was removed through protonation, and the intramolecular Micheal reaction didn't take place under the condition of $0.25 \text{ mol L}^{-1} \text{ H}_2\text{SO}_4$. The one-electron oxidation of the amino group turned into its corresponding cation radical and forms a carbon–nitrogen linkage in $0.25 \text{ mol L}^{-1} \text{ H}_2\text{SO}_4$ [54]. The peak of DOPA by the diffusion controlled with the reduction of DOPA in the across the free hydroxyl groups with two electrons transferred. The carboxylic group of DOPA reacted with the amine group of the polymer (PEDOT-

Boc-Phe or PEDOT-Phe) onto the GCE in the interface, and that the amine groups that were exposed to the solution generate the enantioselectivity.



Scheme 2. Schematic representation of the mechanism for modified glassy carbon electrode with PEDOT-Phe and its consequent enantioselective recognition with DOPA in acid solution.

4. CONCLUSIONS

Chiral EDOT-Boc-Phe and EDOT-Phe were firstly synthesized and electropolymerized for the preparation of corresponding chiral polymers in $\text{CH}_2\text{Cl}_2\text{-Bu}_4\text{NPF}_6$ (0.1 M) system. A series of characterizations were systematically tested for monomers and polymers. The obtained chiral PEDOT-Boc-Phe and PEDOT-Phe films showed good redox activity, and excellent surface structure. Importantly, chiral PEDOT-Boc-Phe and PEDOT-Phe modified electrodes were successful in achieving the goal of distinguishing DOPA enantiomers with the help of sulphuric acid, and SWV has played a significant role in this sensing strategy. The features of the approach were simplicity, rapidity and sensitivity. The method played a vital role for the chiral recognition of various biomolecules.

ACKNOWLEDGEMENTS

The authors would like to acknowledge the financial support of this work by the National Natural Science Foundation of China (51263010, 51303073, 51272096), Natural Science Foundation of Jiangxi Province (20122BAB216011, 20142BAB206028) and the Science and Technology Landing Plan of Universities in Jiangxi province (KJLD14069).

References

1. H. L. Guo, C. M. Knobler, R. B. Kaner, *Synth. Met.* 101 (1999) 44.
2. J. C. Moutet, E. Saintaman, F. Tranvan, P. Angibeaud, J. P. Utille, *Adv. Mater.* 4 (1992) 511.

3. P. A. Bross, U. Schöberl, J. Daub, *Adv. Mater.* 3 (1991) 198.
4. M. M. Green, N. C. Peterson, T. Sato, A. Teramoto, R. Cook, S. Lifson, *Science* 268 (1995) 1860.
5. J. Huang, V. M. Egan, H. Guo, J. Y. Yoon, A. L. Briseno, I. E. Rauda, R. L. Carrell, C. M. Knobber, F. Zhou, R. B. Kaner, *Adv. Mater.* 15 (2003) 1158.
6. Y. Okamoto, E. Yashima, *Angew. Chem., Int. Ed.* 37 (1998) 1020.
7. S. Fireman-Shoresh, I. Popov, D. Avnir, S. Marx, *J. Am. Chem. Soc.* 127 (2005) 2650.
8. L. A. P. Kane-Maguire and G. G. Wallace, *Chem. Soc. Rev.* 39 (2010) 2545.
9. D. Caras-Quintero, P. Bäuerle, *Chem. Commun.* (2004) 926.
10. Y. Sulaiman, R. Katakya, *Analyst* 137 (2012) 2386.
11. (a) H. Goto, Y. S. Jeong, K. Akagi, *Macromol. Rapid Commun.* 26 (2005) 164. (b) Y. S. Jeong, H. Goto, S. Iimura, T. Asano, K. Akagi, *Curr. Appl. Phys.* 6 (2006) 960. (c) H. Goto, K. Akagi, *Macromol. Rapid Commun.* 25 (2004) 1482. (d) H. Goto, K. Akagi, *Macromolecules* 38 (2005) 1091.
12. Y. S. Jeong, K. Akagi, *Macromolecules* 44 (2011) 2418.
13. H. Goto, and K. Akagi, *Chem. Mater.* 18 (2006) 255.
14. S. Matsushita, B. Yan, S. Yamamoto, Y. S. Jeong, and K. Akagi, *Angew. Chem. Int. Ed.* 53 (2014) 1659.
15. J. Park, M. Goh, and K. Akagi, *Macromolecules* 47 (2014) 2784.
16. D. F. Hu, B. Y. Lu, X. M. Duan, J. K. Xu, L. Zhang, K. X. Zhang, S. M. Zhang and S. J. Zhen, *RSC Adv.* 4 (2014) 35597.
17. B. Y. Lu, Y. Lu, Y. P. Wen, X. M. Duan, J. K. Xu, S. Chen, L. Zhang, *Int. J. Electrochem. Sci.* 8 (2013) 2826.
18. Y. Sulaiman and R. Katakya, *Analyst* 137 (2012) 2386.
19. W. Poewe, A. Antonini, J. C. Zijlmans, P. R. Burkhard, F. Vingerhoets, *Clin. Interv. Aging.* 5 (2010) 229.
20. G. Pezzoli, M. Zini, *Expert Opin. Pharmacother.* 11 (2010) 627.
21. G. Cotzias, C. P. Papavasi and R. Gellene, *N. Engl. J. Med.* 280 (1969) 337.
22. R. Krishnaveni, V. Rathod, M. S. Thakur, Y. F. Neelgund, *Curr. Microbiol.* 58 (2009) 12.
23. S. G. Lee, S. P. Hong, M. H. Sung, *Enzyme. Microb. Technol.* 25 (1999) 268.
24. D. F. Reinhold, T. Utne, N. L. Abramson, *US patent*, (1987) 4716246.
25. T. Alexander, C. E. Sortwell, C. D. Sladek, R. H. Roth, K. Steece-Collier, *Cell Transplant.* 6 (1997) 309.
26. A. S. D. Spiers, *Aust. N. Z. J. Med.* (1974) 475.
27. J. Moses, A. Siddiqui, and P. B. Silverman, *Neurosci. Lett.* 218 (1996) 145.
28. L. S. Chen, F. X. Chang, L. C. Meng, M. X. Li and Z. W. Zhu, *Analyst* 139 (2014) 2243.
29. M. Wu, X. J. Zhou, R. Konno, and Y. X. Wang, *Clin. Exp. Pharmacol. Physiol.* 33 (2006) 1042.
30. G. Grigorean, and C. B. Lebrilla, *Anal. Chem.* 73 (2001) 1684.
31. M. Dolezalova, and M. Tkaczykova, *Chirality* 11 (1999) 394.
32. B. Yuan, H. Wu, T. Sanders, C. McCullum, Y. Zheng, P. B. Tchounwou and Y. M. Liu, *Anal. Biochem.* 2011 (416) 191.
33. C. Borst, and U. Holzgrabe, *J. Chromatogr. A* 1204 (2008) 191.
34. M. Blanco, and I. J. Valverde, *Pharm. Biomed. Anal.* 31 (2003) 431.
35. M.K. Lee, A. P. Kumar, D. Jin, and Y. I. Lee, *Rapid Commun. Mass Spectrom.* 22 (2008) 909.
36. Y. J. Kang, J. W. Oh, Y. R. Kim, J. S. Kim, and H. Kim, *Chem. Commun.* 46 (2010) 5665.
37. M. Matsunaga, T. Nakanishi, T. Asahi, and T. Osaka, *Chirality* 19 (2007) 295.
38. M. Matsunaga, T. Nakanishi, T. Asahi, and T. Osaka, *Electrochem. Commun.* 9 (2007) 725.
39. L. Zhang, Y. P. Wen, Y. Y. Yao, X. M. Duan, J. K. Xu, X. Q. Wang, *J. Appl. Polym. Sci.* 130 (2013) 2660.
40. J. L. Segura, R. Gómez, E. Reinold, and P. Bäuerle, *Org. Lett.* 7 (2005) 2345.
41. C. D. McTiernan, M. Chahma, *Synth. Met.* 161 (2011) 1532.

42. A. J. Downard, D. Pletcher, *J. Electroanal. Chem.* 206 (1986) 139.
43. A. J. Downard, D. Pletcher, *J. Electroanal. Chem.* 206 (1986) 147.
44. R. E. Nofhle, D. Pletcher, *J. Electroanal. Chem.* 227 (1987) 229.
45. H. Randriamahazaka, V. Noël, C. Chevrot, *J. Electroanal. Chem.* 472 (1999) 103.
46. M. Zhou, J. Heinze, *Electrochim. Acta.* 44 (1999) 1733.
47. G. Inzelt, M. Pineri, J. W. Schultze, M. A. Vorotyntsev, *Electrochim. Acta.* 45 (2000) 2403.
48. J. X. Zhang, C. Liu, G. Q. Shi, Y. F. Zhao, *J. Polym. Sci. Part B: Polym. Phys.* 43 (2005) 241.
49. H. J. Bowley, D. L. Gerrard, W. F. Maddams, M. R. Paton, *Makromol. Chem.* 186 (1985) 695.
50. B. Y. Lu, J. Yan, J. K. Xu, S. Y. Zhou, X. J. Hu, *Macromolecules* 43 (2010) 4599.
51. A. Brun, R. Rosset, *J. Electroanal. Chem.* 49 (1974) 287.
52. E. Bustos, Luis A. Godínez, G. Rangel-Reyes, E. Juaristi, *Electrochimica. Acta.* 54 (2009) 6445.
53. Y. H. Huang, Q. Han, Q. Zhang, L. J. Guo, *Electrochimica. Acta.* 113 (2013) 564.
54. M. Eslami, M. Namazian, H. R. Zare, *Electrochimica. Acta.* 88 (2013) 543.

© 2015 The Authors. Published by ESG (www.electrochemsci.org). This article is an open access article distributed under the terms and conditions of the Creative Commons Attribution license (<http://creativecommons.org/licenses/by/4.0/>).